Supplemental Methods

Antibodies. The antibodies used were anti-SIRT1 (Santa Cruz Biotechnology for the immunostaining of NRVM or the antibody described previously (1) for all other experiments), anti-MnSOD (Upstate), anti-fibronectin (Serotec), anti-catalase (Sigma), anti-GAPDH (Chemicon), anti histone H3 (Upstate), and anti-acetyl histone H3 (Calbiochem). Anti-histone H3 and anti-acetyl histone H3 antibodies recognize, respectively, the C-terminus of histone H3 and the N-terminal 20 amino acid residues of histone H3 with di-acetylation on lysine 9 and lysine 14. The secondary antibodies were Alexa Fluor 488- or Alexa Fluor 594-conjugated goat anti-rabbit antibody (Molecular Probes). Actin and nuclei were stained with TRITC- or FITC-labeled phalloidin (Sigma) and Hoechst 33342, respectively.

Quantification of nuclear SIRT1, left ventricular fibrosis and MnSOD protein in immunostaining images. The levels of nuclear SIRT1, left ventricular fibrosis and MnSOD protein were evaluated using image analysis software (Adobe Photoshop CS4, Adobe). The ratio of the number of pixels that were positive for both SIRT1 and Hoeschst 33342 staining to the number of pixels that were positive for Hoechst 33342 staining was used as an index for the nuclear accumulation of SIRT1. The ratio of the number of pixels that were positive for fibronectin staining to the number of pixels that were positive for actin staining was used as an index of left ventricular fibrosis. The amount of Mn-SOD protein was quantified as the number of pixels that were positive for Mn-SOD staining per cell.

Plasmid construction. To construct the SIRT1-EGFP fusion protein, the coding region of mouse SIRT1 cDNA lacking its stop codon was cloned into the vector pEGFP-N3 (Clontech) at the XhoI and SalI sites and in-frame with the EGFP coding region. Site-directed mutagenesis was carried out using a QuikChange XL mutagenesis kit (Stratagene).

siRNAs. The sense and anti-sense siRNAs in the cocktail were as follows: CCCUAAGGGUGGUGGAGAAtt (sense) / UUCUCCACCACCCUUAGGGtt (anti-sense), GGAGAAUGUUACUGAAAGAtt (sense) / UCUUUCAGUAACAUUCUCCtt (anti-sense) and GCGCAUACUCUGUGUGAAUtt (sense) / AUUCACACAGAGUAUGCGCtt (anti-sense) for Mn-SOD, and GAACAAAGUUGACGAUUUAtt (sense) / UAAAUCGUCAACUUUGUUCtt (anti-sense), GCAGAAACAGUGAGAAAAUtt (sense) / AUUUUCUCACUGUUUCUGCtt (anti-sense) and GCUCAGAGUUUGAGCAUAUtt (sense) / AUAUGCUCAAACUCUGAGCtt (anti-sense) for SIRT1, respectively.

Rat myocardial infarction model. Male Wistar rats (Sankyo Labo Service), 8-10 weeks old, were anesthetized with a mixture of ketamine (90 mg/kg i.p.) and xylazine (10 mg/kg i.p.),

intubated with an endotracheal tube, and ventilated using a Harvard respirator (model 683; Harvard Apparatus Inc., South Natick, MA) with supplemented oxygen. After a left thoracotomy, a 5.0 silk thread was passed around a marginal branch of the left coronary artery. The rats were then divided into two groups: a sham and a myocardial infarction (MI) group. In the sham group, the coronary artery was not ligated. In the MI group, the coronary branch was permanently ligated to induce myocardial infarction. The surgical wounds were repaired and the rats were returned to their cages for recovery. Four weeks after surgery, the MI group had developed heart failure (2).

Cell culture. To isolate NRVMs, the hearts from 5- to 7-day-old rats were rapidly excised, and the great vessels and atria were removed in Krebs-Henseleit solution at room temperature. Ventricles were transferred to Ca^{2+}-free Krebs-Henseleit solution to remove any extracellular Ca^{2+} and then cut sagittally into four pieces using micro-scissors. The pieces were digested with collagenase (5 mg/ml, Wako Pure Chemical Industries) in a shaking incubator bath (80 rpm) for 60 min at 37°C. The digested tissues were transferred to Krebs-Henseleit solution and gently triturated using a Pasteur pipette. The suspension was filtered through a 70-μm nylon filter, the cells were plated, and the fibroblasts were allowed to adhere to the plate during a subsequent 90-min incubation. The floating cardiomyocytes were collected by centrifugation and cultured. NRVMs or C2C12 cells were cultured in DMEM (Gibco) supplemented with 10% FBS at 37 ºC under 5% CO_2. To detect deacetylated histone H3 *in vitro*, cells were treated with 50 nmol/L tricostatin A for 24 hours to inhibit the activity of class I and class II histone deacetylases.

Measurement of oxidative stress. The levels of cellular oxidative stress was measured using CM-H_2DCFDA (Invitrogen). C2C12 cells or NRVMs were pretreated with 100 μmol/L resveratrol or vehicle for 4 hours and then exposed to ang II for 8 hours or antimycin A for 3 hours, before incubation in 7 μM CM-H_2DCFDA for 10 min. The cells were then fixed with 4% paraformaldehyde and observed by confocal microscopy. The bright green fluorescence of the oxidized DCF probe was quantified using Adobe Photoshop CS4 image analysis software (Adobe): The number of DCF staining-positive pixels per cell was counted and compared among experimental groups.

Assays for apoptosis and LDH activity. Apoptotic cells were detected by staining with Hoechst 33342 or the TUNEL procedure, using an Apoptosis in situ Detection Kit (Wako), following the manufacturer's instructions. The LDH activity of the culture medium was assayed using CytoTox 96 (Promega).

RNA isolation and RT-PCR. Total RNA was isolated using RNeasy kits (Qiagen). For the first-strand cDNA synthesis, 2 μg of the total RNA was incubated at 42˚C for 1 hr with SuperScript^{TM}II reverse transcriptase (Invitrogen) and oligo $(dT)_{12\text{-}18}$. The PCR amplification was performed using Taq DNA polymerase (New England Biolabs) and the following primer pairs: for rat MnSOD, 5'-ACAAACCTGAGCCCTAAGGGTGGTGGAGAA-3' and 5'-GTAAGCGACCTTGCTCCTTATTGAAGC CAA-3'; for hamster MnSOD, 5'-ACCAAGACGTCATCACAAAAGCACCTCTCC-3' and 5'-GGTGTCTGCAGCTGGGAGCTCATCCTAATA-3'. Following the amplification, aliquots of each PCR product were analyzed by electrophoresis in 1.2% agarose gels. Quantitative analyses were performed using NIH Image software.

Echocardiography. Non-invasive cardiac function assessment was performed by two-dimensional and M-mode echocardiography, in isoflurane-anesthetized TO-2 and control golden hamsters at 30 weeks of age. The hamsters were positioned supine with the front paws wide open, and an ultrasound transmission gel was applied to the precordium. Transthoracic echocardiography was performed using an ultrasound biomicroscopy system (Vevo 770, Visualsonics, Toronto) equipped with a 40-MHz mechanical transducer. The left ventricular systolic function was estimated from the left ventricular ejection fraction and the fractional shortening.

References

1. Sakamoto, J., Miura, T., Shimamoto, K., and Horio, Y. (2004) *FEBS Lett* **556**, 281-286.
2. Miki, T., Miura, T., Yano, T., Takahashi, A., Sakamoto, J., Tanno, M., Kobayashi, H., Ikeda, Y., Nishihara, M., Naitoh, K., Ohori, K., and Shimamoto, K. (2006) *J Pharmacol Exp Ther* **317**, 68-75

Supplemental Figure. 1

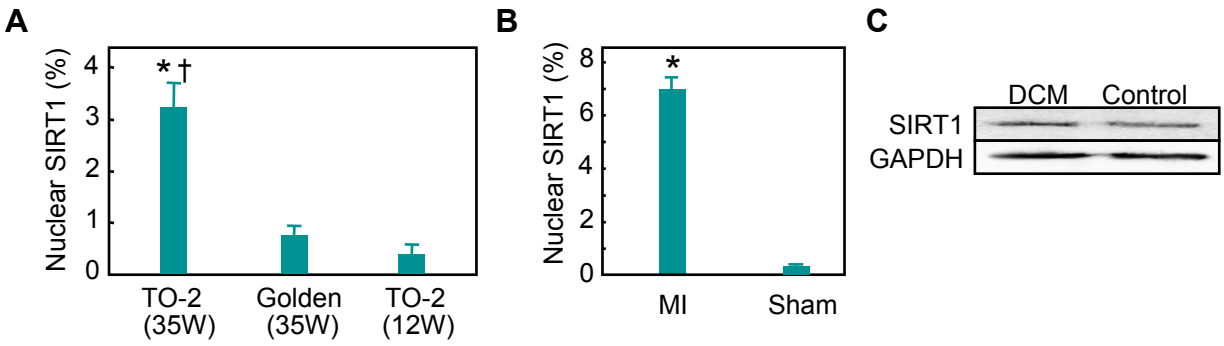

Nuclear expression of SIRT1 in failing hearts. **A** and **B**, The number of cardiomyocytes expressing SIRT1 exclusively in the nucleus was quantified in 35-week old TO-2 hamsters, golden hamsters and 12-week old TO-2 hamsters (**A**) and in non-necrotic, viable areas of rat hearts 4 weeks after myocardial infarction (MI) or sham operation (Sham) (**B**). * $p < 0.05$ vs. 35-week-old golden hamsters or sham-operated rats. † $p<0.05$ vs. 12-week-old TO-2 hamsters. **C**, Immunoblots of SIRT1 and GAPDH in left ventricular muscles from a DCM patient and a patient without heart disease.

Supplemental Figure. 2

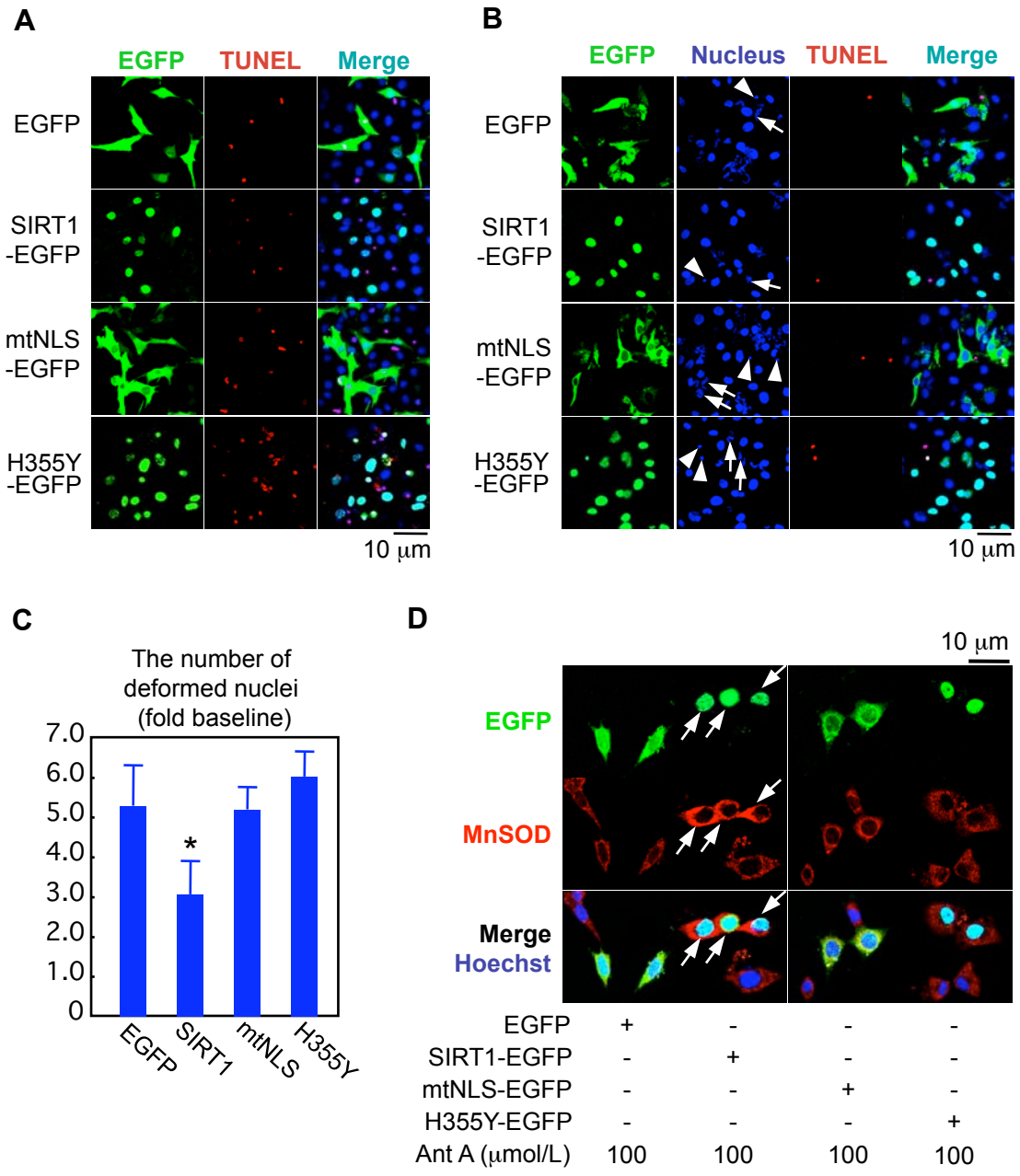

Suppression of cell death and induction of Mn-SOD by nuclear SIRT1. C2C12 cells expressing EGFP, SIRT1-EGFP (nuclear SIRT1), mtNLS-EGFP (cytoplasmic SIRT1), or H355Y-EGFP (dominant-negative SIRT1) were exposed to 100 μmol/L antimycin A (Ant A) for 8 hours. **A**, Representative images of TUNEL-positive staining. Nuclear SIRT1 (SIRT1-EGFP) inhibits apoptosis. **B**, Nuclear SIRT1 (SIRT1-EGFP) inhibits apoptosis and presumably necrosis. Arrowheads and arrows indicate apoptotic cells with condensed nuclei and necrotic cells with severely deformed nuclei or disrupted membranes, respectively. **C**, The number of cells showing necrotic features after exposure to Ant A were counted and expressed as fold-change from baseline. * $p < 0.05$ vs. EGFP. **D**, Mn-SOD staining in C2C12 cells transfected with each plasmid. Note a higher intensity of Mn-SOD immunostaining in the cells overexpressing nuclear SIRT1 (arrows) compared with other cells.

Supplemental Figure. 3

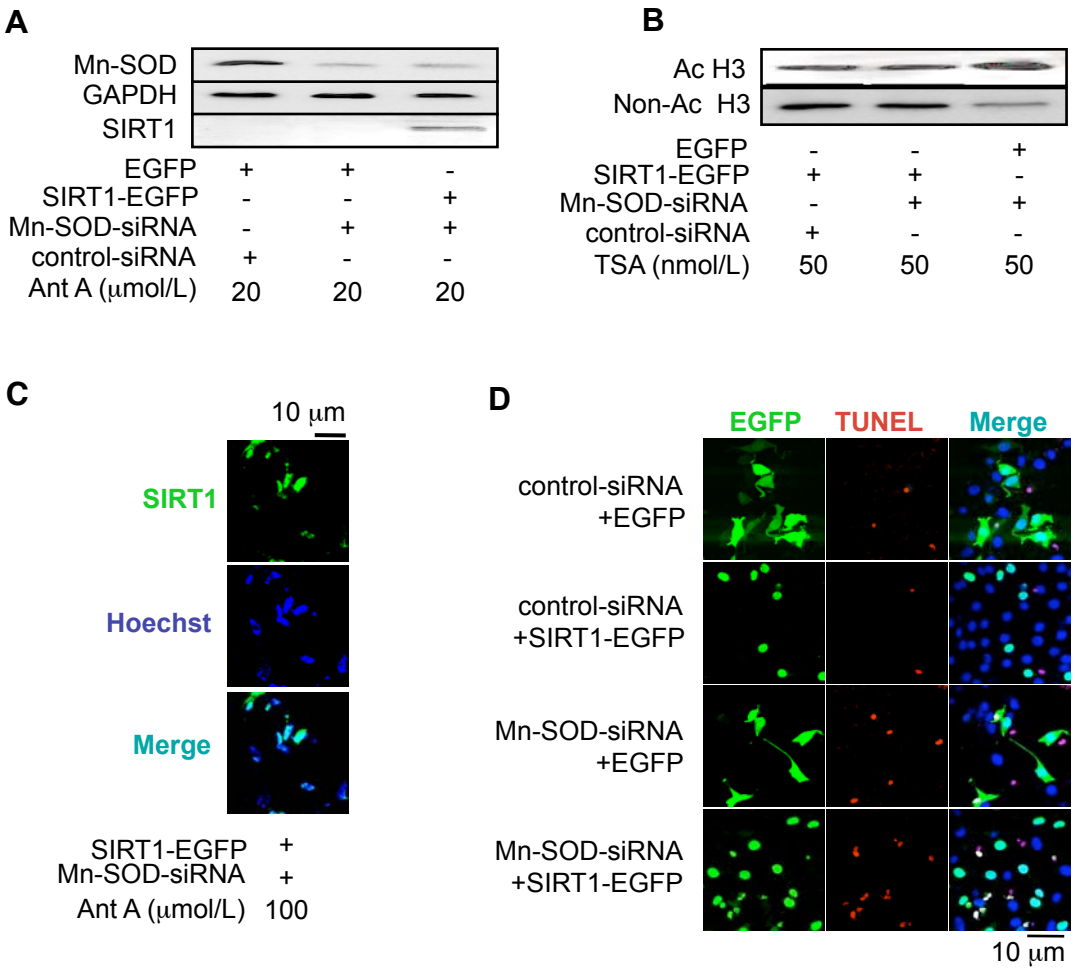

Mn-SOD-siRNA abolishes cell-protective function of nuclear SIRT1. C2C12 cells were transfected with indicated plasmids and/or siRNAs, and were exposed to antimycin A (Ant A) for 12 hours (**A** and **D**) or treated with tricostatin A (TSA) for 24 hours (**B**). **A**, Mn-SOD-siRNA reduced the expression level of Mn-SOD by 75% in C2C12 cells. **B**, The deacetylation of histone H3 by SIRT1 was not affected by Mn-SOD-siRNA. Ac H3, acetylated histone H3; Non-Ac H3, deacetylated histone H3. **C**, C2C12 cells transfected with SIRT1-EGFP and Mn-SOD-siRNA were exposed to 100 μmol/L Ant A for 12 hours. Note that most untransfected cells died and had detached from the culture dish, whereas almost all the residual cells expressed SIRT1-EGFP. **D**, Representative images of C2C12 cells exposed to 20 μmol/L antimycin A in the presence or absence of Mn-SOD-siRNA. Note that overexpresion of nuclear SIRT1 failed to rescue cells exposed to Ant A in the presence of Mn-SOD-siRNA.

Supplemental Figure. 4

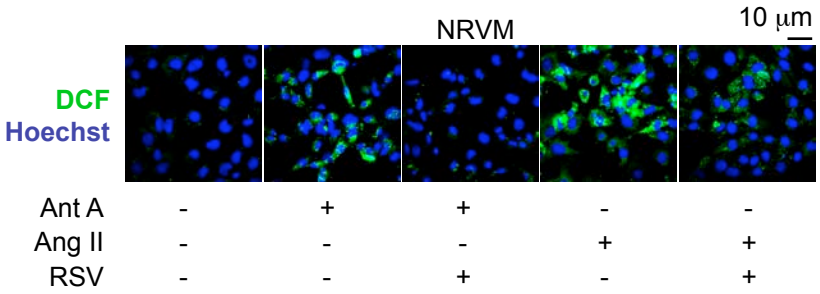

ROS levels measured by DCF fluorescence. NRVMs were pretreated with RSV (100 μmol/L) or vehicle for 4 hours and then exposed to Ant A (100 μmol/L, 3 hours) or angiotensin II (100 μmol/L, 8 hours). Representative images showing anti-oxidative function of RSV are shown.

Supplemental Figure. 5

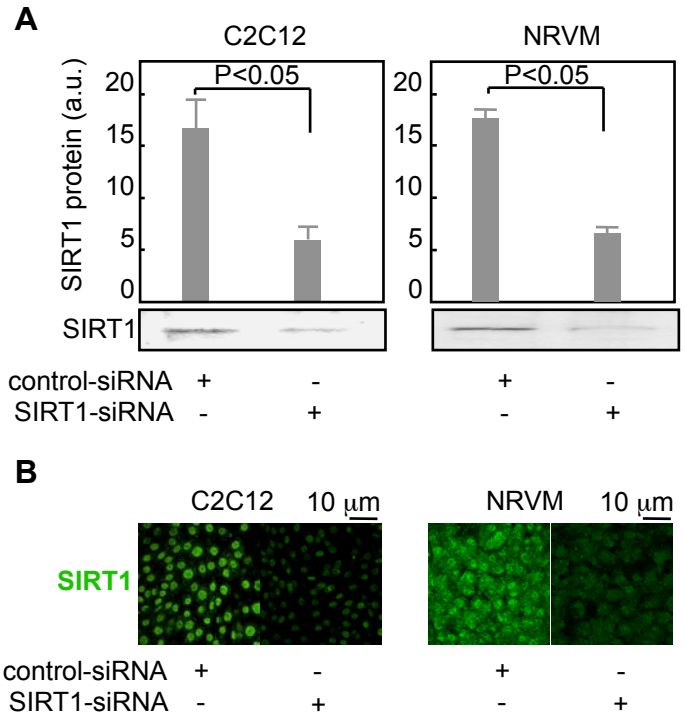

Suppression of SIRT1 expression by SIRT1-siRNA. C2C12 cells (left panels) and NRVMs (right panels) were transfected with either a control-siRNA or SIRT1-siRNA as described in Methods section. Representative immunoblots and the quantitative data from 4 independent series of experiments (**A**) and representative images of SIRT1 immunostaining (**B**) are shown. SIRT1 protein levels were reduced to about 25% of the those in control cells both in C2C12 cells and NRVMs.

Supplemental Figure. 6

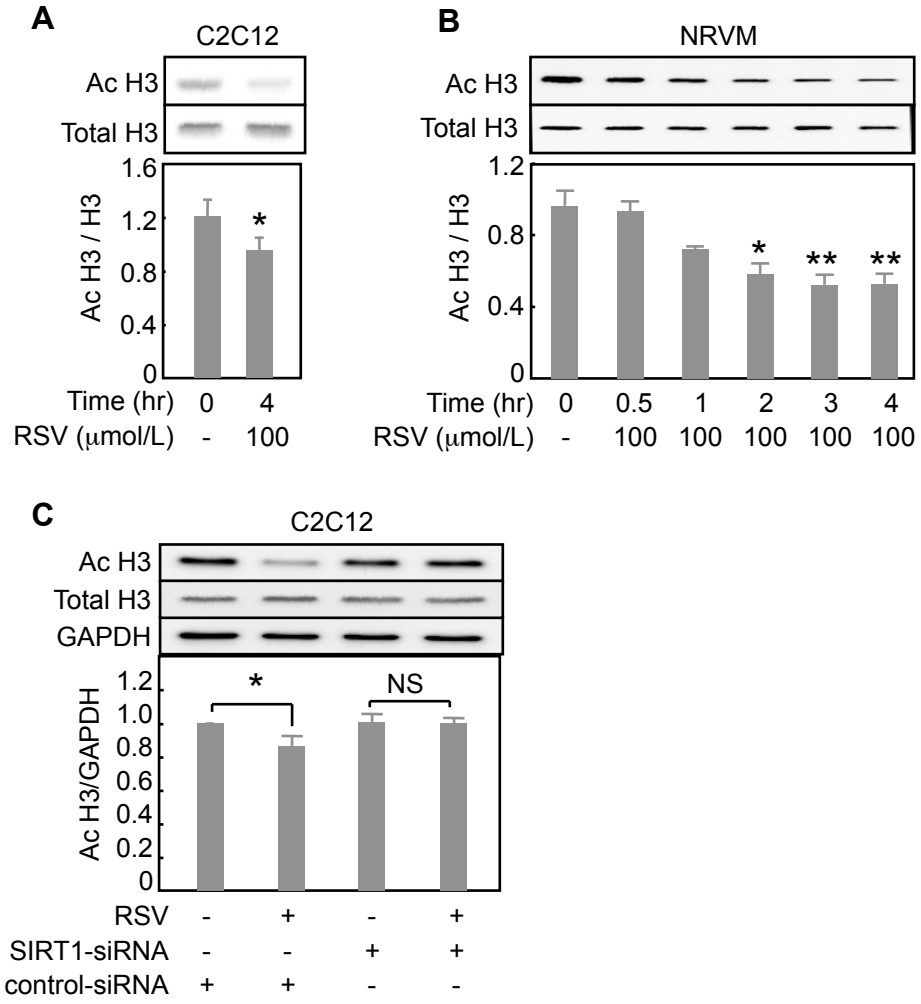

Resveratrol induces deacetylation of histone H3 via SIRT1. **A** and **B**, C2C12 cells or NRVMs were treated with resveratrol (RSV) for the indicated period of time in the presence of tricostatin A and analyzed by immunoblots. **C**, C2C12 cells expressing SIRT1-siRNA or control-siRNA were treated with RSV or vehicle for 4 hours. Ac H3, acetyl histone H3. * $p < 0.05$ and ** $p < 0.01$ vs. untreated control cells. NS, no significant difference.

Supplemental Figure. 7

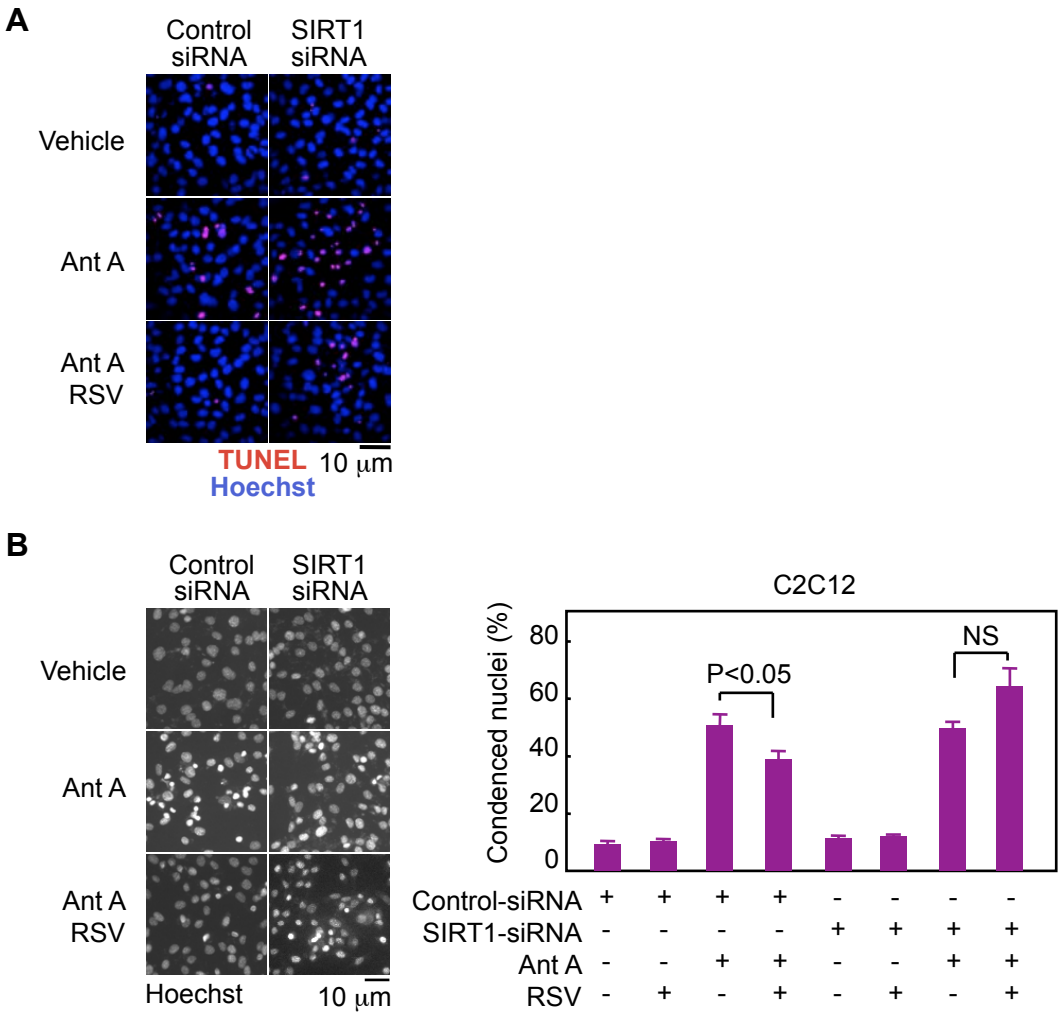

SIRT1-siRNA inhibits the anti-apoptotic function of resveratrol. **A**, NRVMs expressing SIRT1-siRNA or control-siRNA were pretreated with 100 μmol/L of resveratrol (RSV) or vehicle for 4 hours, and then exposed to 100 μmol/L of antimycin A (Ant A) for 8 hours. The representative images of TUNEL staining are shown. **B**, C2C12 cells expressing SIRT1-siRNA or control-siRNA were pretreated with RSV (100 μmol/L) or vehicle for 4 hours, and then exposed to antimycin A (Ant A) (100 μmol/L, 8 hours). Apoptotic cells were identified by condensed nuclear staining with Hoechst 33342. Representative images of nuclear condensation (white nuclei) and their percentage from five independent series of experiments are shown.

Supplemental Figure. 8

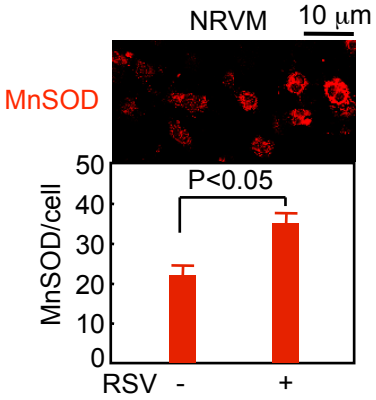

Resveratrol upregulates Mn-SOD in NRVMs. NRVMs were treated with RSV (100 μmol/L) or vehicle for 4 hours and then exposed to100 μmol/L of antimycin A for 3 hours. Representative immunostaining images and their quantitative analysis from 4 independent series of experiments are shown.

Supplemental Figure. 9

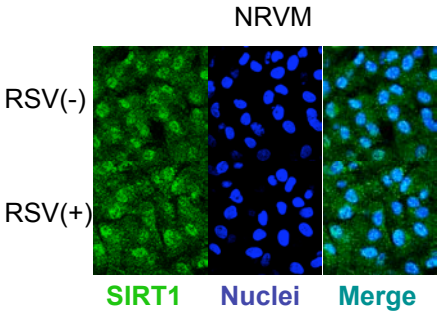

Resveratrol affected neither subcellular localization nor expression levels of SIRT1. NRVMs were immunostained with anti-SIRT1 antibody (green) and Hoechst 33342 (nucleus/blue) before or after treatment with 100 μmol/L of resveratrol for 8 hours.

Supplemental Figure. 10

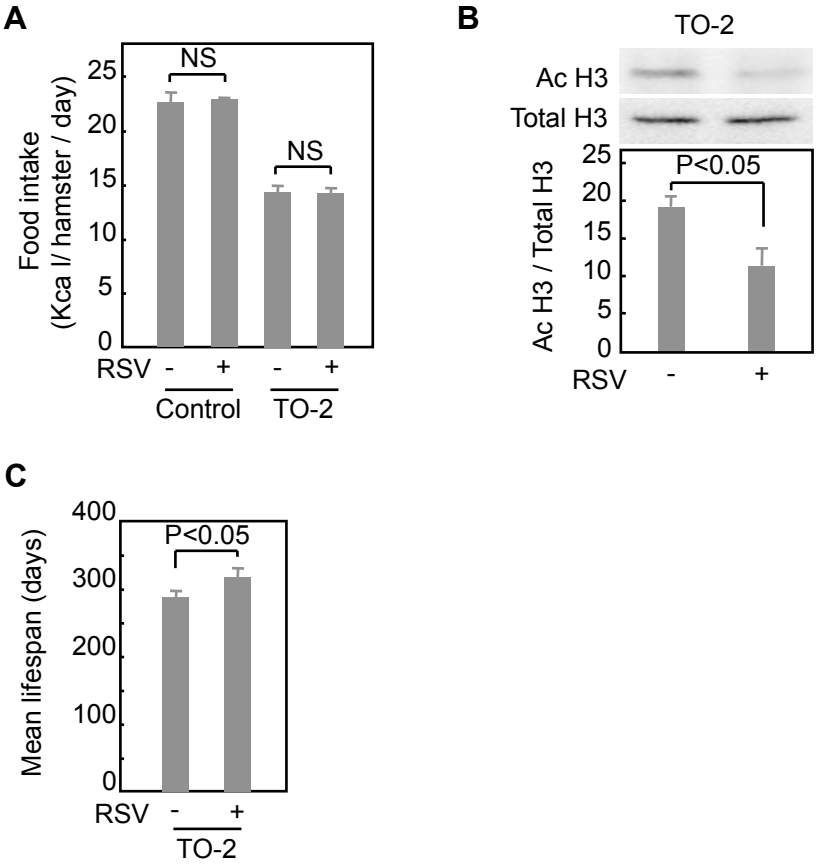

A, Average daily calorie intake was similar between hamsters fed the control diet and those fed resveratrol (RSV)-containing diet. The amount of food consumed by individual hamsters was measured from the age of 25 weeks to 30 weeks. **B**, Resveratrol reduces the levels of acetyl histone H3 in the left ventricle of TO-2 hamsters. Representative immunoblots from left vetricles of 35-week-old TO-2 hamsters and quantitative analyses of the data from four hamsters in each group are shown. **C**, Mean life span of TO-2 hamsters. Oral administration of resveratrol significantly prolonged the average life span of TO-2 hamsters from 287±10 to 318±13 days.